

# Revisiting the hypertriton lifetime puzzle

A. Pérez-Obiol<sup>a</sup>, D. Gazda<sup>b</sup>, E. Friedman<sup>c</sup>, A. Gal<sup>c,\*</sup>

<sup>a</sup>Laboratory of Physics, Kochi University of Technology, Kami, Kochi 782-8502, Japan

<sup>b</sup>Nuclear Physics Institute, 25068 Řež, Czech Republic

<sup>c</sup>Racah Institute of Physics, The Hebrew University, Jerusalem 91904, Israel

---

## Abstract

Conflicting values of the hypertriton ( ${}^3_{\Lambda}\text{H}$ ) lifetime were extracted in recent relativistic heavy-ion collision experiments. The ALICE Collaboration's reported  ${}^3_{\Lambda}\text{H}$  lifetime  $\tau({}^3_{\Lambda}\text{H})$  is compatible within measurement uncertainties with the free  $\Lambda$  lifetime  $\tau_{\Lambda}$ , as naively expected for a loosely bound  $\Lambda$  hyperon in  ${}^3_{\Lambda}\text{H}$ , whereas STAR's reported range of  $\tau({}^3_{\Lambda}\text{H})$  values is considerably shorter:  $\tau_{\text{STAR}}({}^3_{\Lambda}\text{H}) \sim (0.4-0.7)\tau_{\Lambda}$ . This  ${}^3_{\Lambda}\text{H}$  lifetime puzzle is revisited theoretically, using  ${}^3_{\Lambda}\text{H}$  three-body wavefunctions generated in a chiral effective field theory approach to calculate the decay rate  $\Gamma({}^3_{\Lambda}\text{H} \rightarrow {}^3\text{He} + \pi^-)$ . Significant but opposing contributions arise from  $\Sigma NN$  admixtures in  ${}^3_{\Lambda}\text{H}$  and from  $\pi^-$ - ${}^3\text{He}$  final-state interaction. Evaluating the inclusive  $\pi^-$  decay rate  $\Gamma_{\pi^-}({}^3_{\Lambda}\text{H})$  via a branching ratio  $\Gamma({}^3_{\Lambda}\text{H} \rightarrow {}^3\text{He} + \pi^-) / \Gamma_{\pi^-}({}^3_{\Lambda}\text{H})$  determined in helium bubble-chamber experiments, and adding  $\Gamma_{\pi^0}({}^3_{\Lambda}\text{H})$  through the  $\Delta I = \frac{1}{2}$  rule, we derive  $\tau({}^3_{\Lambda}\text{H})$  assuming several different values of the  $\Lambda$  separation energy  $B_{\Lambda}({}^3_{\Lambda}\text{H})$ . It is concluded that each of ALICE and STAR reported  $\tau({}^3_{\Lambda}\text{H})$  intervals implies its own constraint on  $B_{\Lambda}({}^3_{\Lambda}\text{H})$ :  $B_{\Lambda} \lesssim 0.1$  MeV for ALICE,  $B_{\Lambda} \gtrsim 0.2$  MeV for STAR.

*Keywords:* few-body  $\Lambda$  hypernuclei;  ${}^3_{\Lambda}\text{H}$  lifetime experiments and calculations; EFT hyperon-nucleon forces.

---

## 1. Introduction

The hypertriton,  ${}^3_{\Lambda}\text{H}$ , a  $\Lambda pn$  bound state with isospin  $I=0$  and spin-parity  $J^P = \frac{1}{2}^+$ , is the lightest bound  $\Lambda$  hypernucleus [1]. Given the tiny  $\Lambda$  separation

---

\*corresponding author: Avraham Gal, avragal@savion.huji.ac.il

energy  $B_\Lambda(^3\Lambda\text{H})=0.13\pm 0.05$  MeV [2], implying a  $\Lambda$ -deuteron mean distance of about 10 fm, the  $^3\Lambda\text{H}$  decay rate is expected to be close to that of the free  $\Lambda$  hyperon which to 99.7% is governed by the nonleptonic  $\Lambda\rightarrow N\pi$  weak-decay mode. This expectation was quantified using a  $3N$  final-state closure approximation in early  $^3\Lambda\text{H}$  lifetime calculations [3] leading to an estimate  $\Gamma(^3\Lambda\text{H})/\Gamma_\Lambda=1+0.14\sqrt{B_\Lambda}$  ( $B_\Lambda$  in MeV), thereby suggesting a roughly 5% enhanced  $^3\Lambda\text{H}$  decay rate  $\Gamma(^3\Lambda\text{H})$  with respect to the free  $\Lambda$  decay rate  $\Gamma_\Lambda$ , i.e.  $\tau(^3\Lambda\text{H})\approx 0.95\tau_\Lambda$ . Yet values of  $\tau(^3\Lambda\text{H})$  considerably shorter than  $\tau_\Lambda$  were reported recently by two of the three relativistic heavy ion (RHI) experiments (HypHI and STAR) listed in Table 1, in distinction from ALICE most recent values which within their own uncertainties agree with  $\tau_\Lambda$  [9, 10]. In fact, a similarly large spread of  $\tau(^3\Lambda\text{H})$  values, and with bigger uncertainties, had been reported in old nuclear emulsion and helium bubble-chamber (BC) hypernuclear measurements [14]. Finally, as if to compound confusion, STAR just published a  $B_\Lambda(^3\Lambda\text{H})$  range of values much higher than listed above [15, 16]. Implications to  $A\leq 7$  hypernuclei are discussed in Ref. [17]. A more precise determination of  $B_\Lambda(^3\Lambda\text{H})$  may constrain the balance between two-body hyperon-nucleon ( $YN$ ) and three-body  $YNN$  forces which at densities higher than met in hypernuclei is at the heart of the so called hyperon puzzle in neutron stars, i.e. the difficulty to reconcile recent observations of  $\sim 2M_\odot$  neutron stars with having hyperons in their interior [18, 19]; see Ref. [20] for a recent review.

Table 1:  $^3\Lambda\text{H}$  lifetime values  $\tau(^3\Lambda\text{H})$  in ps from recent RHI experiments and from post-97 published, or to be published calculations. Note:  $\tau_\Lambda=263\pm 2$  ps [4].

Exp/Th	Collaboration	$\tau(^3\Lambda\text{H})$
Exp	HypHI [5]	$183_{-32}^{+42}\pm 37$ [5]
Exp	STAR [6, 7]	$142_{-21}^{+24}\pm 29$ [7]
Exp	ALICE [8, 9, 10]	$242_{-38}^{+34}\pm 17$ [9]
Th	Kamada et al. [11]	256
Th	Gal-Garcilazo [12]	$213\pm 5$
Th	Hildenbrand-Hammer [13]	$\approx \tau_\Lambda$

Table 1 also lists post-1997  $\tau(^3\Lambda\text{H})$  calculations known to us. The first calculation [11] derived a value shorter by a few percent than  $\tau_\Lambda$  in a complete Faddeev calculation, dealing with *all* three  $\pi^-$  final-state channels:  $^3\text{He}\pi^-$ ,

$dp\pi^-$  and  $ppn\pi^-$ , while using the  $\Delta I = \frac{1}{2}$  rule to add the  $\pi^0$  decay channels. However, the  $YN$  SC89 Nijmegen interaction [21] used there to construct a three-body  ${}^3_\Lambda\text{H}$  wavefunction does poorly in hypernuclei, beginning with  $A=4$  [22]. The second calculation [12] derived a  $\tau({}^3_\Lambda\text{H})$  value shorter than  $\tau_\Lambda$  by  $\sim 20\%$ , half of which from attractive final-state interaction (FSI) of the outgoing pion. The third calculation [13] is perhaps oversimplified by treating  ${}^3_\Lambda\text{H}$  and  ${}^3\text{He}-{}^3\text{H}$  as  $\Lambda d$  and  $Nd$  loosely bound two-body systems, respectively.

In this Letter we report on a new evaluation of the partial decay rate  $\Gamma({}^3_\Lambda\text{H} \rightarrow {}^3\text{He} + \pi^-)$  using  ${}^3_\Lambda\text{H}$  wavefunctions from a chiral effective field theory ( $\chi\text{EFT}$ ) leading-order (LO)  $YN$  interaction model [23, 24] applied successfully in *ab initio* calculations of  $A=3,4$  hypernuclear binding energies [25, 26, 27]. Surprisingly, the  $\lesssim 0.5\%$  norm  $\Sigma NN$  admixtures reduce by  $\approx 10\%$  the purely  $\Lambda NN$  decay rate. In contrast, using realistic low-energy  $\pi^-{}^3\text{He}$  distorted waves (DW) rather than plane waves (PW) enhances  $\Gamma({}^3_\Lambda\text{H} \rightarrow {}^3\text{He} + \pi^-)$  by  $\approx 15\%$ . The inclusive  $\pi^-$  decay rate  $\Gamma_{\pi^-}({}^3_\Lambda\text{H})$  is then obtained using the BC world average branching ratio  $R_3 = \Gamma({}^3_\Lambda\text{H} \rightarrow {}^3\text{He} + \pi^-) / \Gamma_{\pi^-}({}^3_\Lambda\text{H}) = 0.35 \pm 0.04$  [14]. Adding the inclusive  $\pi^0$  decay rate,  $\Gamma_{\pi^0}({}^3_\Lambda\text{H}) = \frac{1}{2}\Gamma_{\pi^-}({}^3_\Lambda\text{H})$  by the  $\Delta I = \frac{1}{2}$  rule, we provide a new theoretical statement about  $\tau({}^3_\Lambda\text{H})$  and its relationship to  $B_\Lambda({}^3_\Lambda\text{H})$  for each of the three RHI experiments listed in Table 1.

## 2. Form Factors

To relate  $\Gamma({}^3_\Lambda\text{H} \rightarrow {}^3\text{He} + \pi^-)$  to the free- $\Lambda$  partial decay rate  $\Gamma(\Lambda \rightarrow p\pi^-)$  we follow Kamada et al. [11], Eq. (A5), writing  $\Gamma(\Lambda \rightarrow p\pi^-)$  in the form

$$\frac{\Gamma_{\Lambda \rightarrow p\pi^-}}{(G_F m_\pi^2)^2} = \frac{k_{\pi^-}}{\pi} \frac{M_p}{M_p + \omega_{\pi^-}} \left[ \mathcal{A}_\Lambda^2 + \mathcal{B}_\Lambda^2 \left( \frac{k_{\pi^-}}{2\bar{M}} \right)^2 \right], \quad (1)$$

with  $k_{\pi^-} = 100.6$ ,  $\omega_{\pi^-} = 172.0$ ,  $\bar{M} = \frac{1}{2}(M_p + M_\Lambda) = 1027$ , all in MeV, with  $G_F m_\pi^2 = 2.21 \cdot 10^{-7}$ , and where  $\mathcal{A}_\Lambda = 1.024$ ,  $\mathcal{B}_\Lambda = -9.431$  are chosen here to satisfy the new BESIII value of the  $\Lambda \rightarrow p\pi^-$  asymmetry parameter [28]. This gives  $\Gamma(\Lambda \rightarrow p\pi^-) = 2.534$  GHz, and adding half of it for  $\Gamma(\Lambda \rightarrow n\pi^0)$  to respect the  $\Delta I = \frac{1}{2}$  rule yields  $\tau_\Lambda \approx \tau(\Lambda \rightarrow N\pi) = \Gamma^{-1}(\Lambda \rightarrow N\pi) = 263.1$  ps. The squares of  $\mathcal{A}_\Lambda$  and  $\mathcal{B}_\Lambda$  above arise from a  $\Lambda \rightarrow p\pi^-$  parity violating (PV) spin-independent amplitude  $\mathcal{A}_\Lambda$  and a parity conserving (PC) spin-dependent amplitude  $\mathcal{B}_\Lambda \vec{\sigma} \cdot \hat{k}_{\pi^-}$ , respectively. The PV contribution in Eq. (1) dominates with 83% of  $\Gamma(\Lambda \rightarrow p\pi^-)$ .

Proceeding to  $\Gamma({}^3_{\Lambda}\text{H} \rightarrow {}^3\text{He} + \pi^-)$ , we introduce nuclear form factors that accompany the  $\Lambda \rightarrow p\pi^-$  PV and PC decay amplitudes,  $\mathcal{A}_{\Lambda} \rightarrow \mathcal{A}_{\Lambda} F^{\text{PV}}(\vec{q})$  and  $\mathcal{B}_{\Lambda} \vec{\sigma} \cdot \hat{k}_{\pi^-} \rightarrow \mathcal{B}_{\Lambda} F^{\text{PC}}(\vec{q}, \vec{\sigma})$ :

$$\frac{\Gamma_{\Lambda \rightarrow {}^3\text{He} + \pi^-}^3}{(G_F m_{\pi}^2)^2} = 3 \frac{q}{\pi} \frac{M_{3\text{He}}}{M_{3\text{He}} + \omega_{\pi^-}(q)} \left[ \mathcal{A}_{\Lambda}^2 |F^{\text{PV}}(\vec{q})|^2 + \mathcal{B}_{\Lambda}^2 |F^{\text{PC}}(\vec{q}, \vec{\sigma})|^2 \left( \frac{k_{\pi^-}}{2M} \right)^2 \right] \quad (2)$$

where the isospin factor 3 counts the three final nucleons to which the  $\Lambda$  may turn into. Appropriate spin averages and summation are implied. In Eq. (2) the pion c.m. momentum (energy) is  $q=114.4$  ( $\omega_{\pi^-}=179.3$ ),  $M_{3\text{He}}=2809$ , using charge-averaged masses  $M_N=938.92$ ,  $m_{\pi}=138.04$ , all in MeV. The nuclear form factors  $F^j(\vec{q}, \vec{\sigma})$ , where the index  $j$  stands for PV or PC, are defined by

$$F^j(\vec{q}, \vec{\sigma}) = \int \Phi_f^* \phi_{\pi}(\vec{q}; \vec{r}) \mathcal{O}^j(\vec{q}, \vec{\sigma}) \Phi_i d^3 r_3 d^3 R, \quad (3)$$

where  $\mathcal{O}^{\text{PV}} = 1$ ,  $\mathcal{O}^{\text{PC}} = \vec{\sigma} \cdot \hat{q}$ , and  $\Phi_{i,f}(\vec{R}, \vec{r}_3)$  are initial  ${}^3_{\Lambda}\text{H}$  and final  ${}^3\text{He}$  three-body wavefunctions in terms of Jacobi coordinates:  $\vec{R}$  for the relative coordinate of spectator nucleons 1 and 2 and  $\vec{r}_3$  for the coordinate of the third, ‘active’ baryon relative to the c.m. of the spectator nucleons. Spin-isospin variables are kept implicit. The DW  $\pi^-$  wavefunction  $\phi_{\pi}(\vec{q}; \vec{r})$  evolves via FSI from a PW pion with momentum  $\vec{q}$  in the  ${}^3_{\Lambda}\text{H}$  rest frame. Its argument  $\vec{r} = \frac{2}{3}\vec{r}_3$  is identified with the coordinate of the active baryon with respect to the c.m. of  ${}^3\text{He}$ .

New  $\Sigma$ -hyperon two-body decay channels,  $\Sigma^- \rightarrow n\pi^-$  and  $\Sigma^0 \rightarrow p\pi^-$ , become available in  ${}^3_{\Lambda}\text{H} \rightarrow {}^3\text{He} + \pi^-$  once  $\Sigma NN$  admixtures are considered. The corresponding  $\Sigma^-$  decay amplitudes are taken from studies of its weak decay:  $\mathcal{A}_{\Sigma^-} = 1.364$ , fitted to the lifetime value  $\tau_{\Sigma^-} = 147.9 \pm 1.1$  ps [4], and a negligible  $\mathcal{B}_{\Sigma^-}$  [29]. Since the  $\Sigma^0 \rightarrow p\pi^-$  weak decay in free space is superseded by the  $\Sigma^0 \rightarrow \Lambda\gamma$  electromagnetic decay we use the chiral-Lagrangian prediction  $\mathcal{A}_{\Sigma^0} = \frac{1}{\sqrt{2}} \mathcal{A}_{\Sigma^-}$  [29] and neglect  $\mathcal{B}_{\Sigma^0}$ . Using isospin basis consistent with that used in our  ${}^3_{\Lambda}\text{H}$  wavefunction construction, the form factor  $F^{\text{PV}}$  in Eq. (2) is generalized according to:

$$\mathcal{A}_{\Lambda} F^{\text{PV}} \rightarrow \mathcal{A}_{\Lambda} F_{I=0}^{\text{PV}} + \frac{1}{3} (\sqrt{2} \mathcal{A}_{\Sigma^-} + \mathcal{A}_{\Sigma^0}) F_{I=1}^{\text{PV}} = \mathcal{A}_{\Lambda} F_{I=0}^{\text{PV}} + \frac{1}{\sqrt{2}} \mathcal{A}_{\Sigma^-} F_{I=1}^{\text{PV}}, \quad (4)$$

whereas  $\mathcal{B}_{\Lambda} F^{\text{PC}} \rightarrow \mathcal{B}_{\Lambda} F_{I=0}^{\text{PC}}$ . The subscripts  $I = 0, 1$  indicate restricting in Eq. (3) the expansion of the  ${}^3_{\Lambda}\text{H}$  wavefunction  $\Phi_i$  to  $I_{NN} = 0$   $\Lambda NN$  or to

$I_{NN} = 1$   $\Sigma NN$  components, respectively. Since the two PV amplitudes in Eq. (4) interfere upon forming their summed absolute value squared, even as small a  $\Sigma NN$  admixture probability as  $P_{\Sigma} \lesssim 0.5\%$  may affect considerably the calculated  ${}^3_{\Lambda}\text{H}$  two-body  $\pi^-$  decay rate which is found to be *reduced* by slightly over 10% from its value disregarding  $\mathcal{A}_{\Sigma^-}$ .

### 3. Pion Distorted Waves

The DW pion wavefunction  $\phi_{\pi}(\vec{q}; \vec{r})$  input to the form factors  $F^{\text{PV,PC}}(\vec{q})$ , Eq. (3), was generated from a standard optical potential [30, 31]. The low-energy pion-nucleus interaction is well understood in terms of optical potentials constrained by pionic atoms data across the periodic table. Here we used optical potential parameters from large scale fits to  $\pi^-$ -atom level shifts and widths, from Ne to U [32, 33], where  $s$ - and  $p$ -wave  $\pi N$  scattering amplitude parameters associated with optical potential terms linear in the nuclear density come out close to their threshold real on-shell values. Parameters associated with optical potential terms quadratic in density are phenomenological. Applying this potential to pionic atoms of  ${}^3\text{He}$  it is found to reproduce the experimental  $1S$  level shift and width [34].

To extrapolate from near-threshold to  $q=114.4$  MeV in the  $\pi^- {}^3\text{He}$  c.m. system we revised the above  $\pi N$  linear-density terms using scattering amplitudes from the SAID package [35]. As for the non-linear terms, we extrapolated their threshold values by using also fits to  $\pi^{\pm}$  elastic scattering at  $T_{\text{lab}}=21.5$  MeV on Si, Ca, Ni and Zr [36]. This resulted in a practically vanishing value of the  $s$ -wave term and a 65% increase of the  $p$ -wave term.

Expanding  $\phi_{\pi}(\vec{q}; \vec{r})$  in our calculations in partial waves  $\ell_{\pi}$ , and recalling the spin-parity  $J^P=\frac{1}{2}^+$  of both  ${}^3\text{He}$  and  ${}^3_{\Lambda}\text{H}$ , it follows that the only values allowed are  $\ell_{\pi}=0,2$ . Numerically we find a negligible  $\ell_{\pi}=2$  contribution of order 0.1%, proceeding exclusively through the relatively minor PC amplitude which in total contributes  $\lesssim 3\%$  to  $\Gamma({}^3_{\Lambda}\text{H} \rightarrow {}^3\text{He} + \pi^-)$ . For the dominant  $\ell_{\pi}=0$  contribution,  $|F^{\text{PC}}|^2 = \frac{1}{9}|F^{\text{PV}}|^2$  holds to better than 1%.

### 4. $YNN$ Input and $\Gamma({}^3_{\Lambda}\text{H} \rightarrow {}^3\text{He} + \pi^-)$

Three-body wavefunctions of  ${}^3\text{He}$  and  ${}^3_{\Lambda}\text{H}$ , input to  $F^{\text{PV}}$  and  $F^{\text{PC}}$  of Eq. (3), were generated from Hamiltonians based on  $\chi\text{EFT}$  interactions: NNLOsim for  $NN + NNN$ , derived by fitting  $NN$  data up to  $T_{\text{lab}}^{\text{max}}=290$  MeV with a regulator cutoff momentum  $\Lambda_{\text{EFT}}=500$  MeV [37], and LO  $YN$  [23, 24]

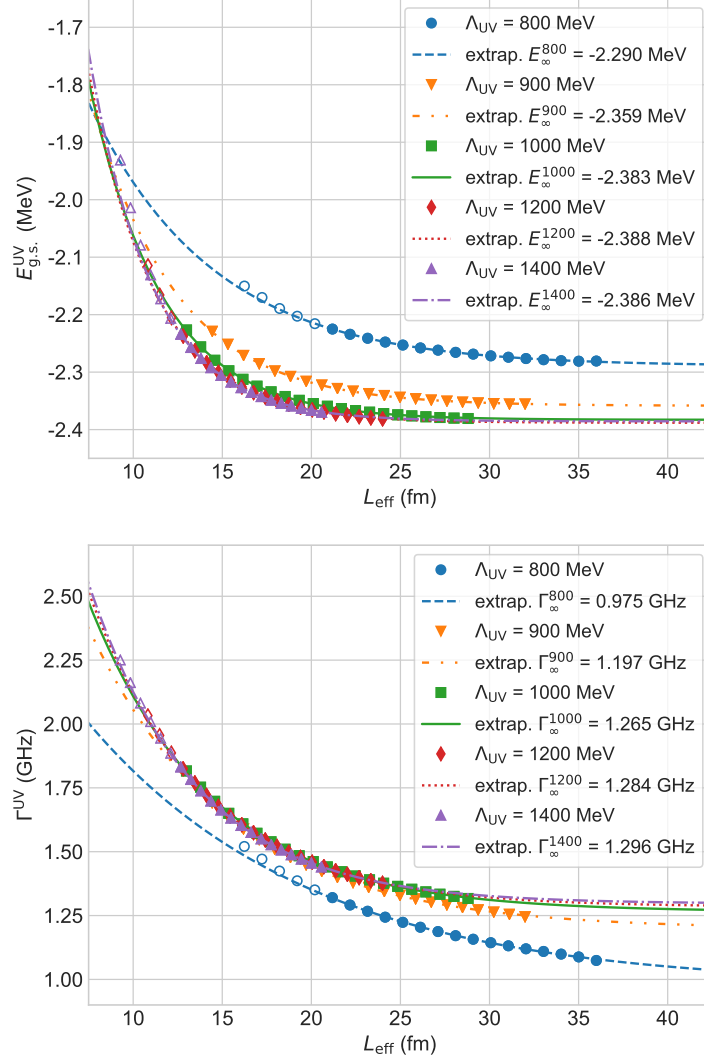


Figure 1: Extrapolations of NCSM calculated  ${}^3_{\Lambda}\text{H}$  ground-state energies  $E_{g.s.}^{UV}(L_{eff})$  (upper) and the corresponding  ${}^3_{\Lambda}\text{H} \rightarrow {}^3\text{He} + \pi^-$  decay rates  $\Gamma^{UV}(L_{eff})$  (lower) as a function of the IR length  $L_{eff}$  using, e.g., Eq. (5) for several fixed UV cutoff values  $\Lambda_{UV}$ .  $N_{max}=36$  and  $\hbar\omega=14$  MeV are held fixed for  ${}^3\text{He}$ . Open symbols start at  $N_{max}=28$ . Filled symbols mark particle-stable  ${}^3_{\Lambda}\text{H}$  configurations included in the fits, starting with a variable  $N_{max}$  between 28 and 40, and up to  $N_{max}=68$ .  $\Sigma NN$  admixtures and DW pions are included in the decay-rate calculations of the lower panel.

with  $\Lambda_{\text{EFT}}=600$  MeV. We followed the *ab initio* no-core shell model (NCSM) method within momentum-space harmonic-oscillator (HO) bases consisting of all excited states limited by  $\mathcal{E}_{\text{HO}} \leq (N_{\text{max}} + 3)\hbar\omega$  for a given HO frequency  $\omega$  [38]. The calculated  ${}^3\text{He}$  ground-state energy converges around  $N_{\text{max}}=30$  to  $E_{\text{exp}}({}^3\text{He})$ , independently of the HO frequency  $\omega$  over a wide range. In contrast, convergence for the weakly bound  ${}^3_{\Lambda}\text{H}$ , down to uncertainty of a few keV, is reached only in the largest NCSM space with  $N_{\text{max}}=70$ . Although the  ${}^3_{\Lambda}\text{H}$  energy computed at  $N_{\text{max}}=70$  exhibits a variational minimum for  $\hbar\omega \approx 9$  MeV, with  $B_{\Lambda}({}^3_{\Lambda}\text{H})=0.16$  MeV, the corresponding  ${}^3_{\Lambda}\text{H} \rightarrow {}^3\text{He} + \pi^-$  decay rates exhibit undesired, stronger dependence on  $\hbar\omega$ . A standard empirical solution to tame such dependence is to extrapolate  $\Gamma_{\hbar\omega}(N_{\text{max}})$ , for a fixed  $\hbar\omega$ , exponentially to  $N_{\text{max}} \rightarrow \infty$ . Here, instead, we applied a recently proposed EFT-inspired extrapolation scheme, introducing infrared (IR) length scale  $L_{\text{eff}}$  and ultraviolet (UV) momentum scale  $\Lambda_{\text{UV}}$  to the NCSM many-body HO bases [39]. Fixing  $\Lambda_{\text{UV}}$  at a sufficiently large value,  $\Lambda_{\text{UV}} \gg \Lambda_{\text{EFT}}$ , the  $\hbar\omega$  and  $N_{\text{max}}$  dependence of  $\Gamma_{\hbar\omega}(N_{\text{max}})$  may be traded off by its IR dependence on  $L_{\text{eff}}$ . Extrapolating then  $\Gamma_{\text{UV}}(L_{\text{eff}})$ , for a fixed  $\Lambda_{\text{UV}}$ , exponentially to  $L_{\text{eff}} \rightarrow \infty$ ,

$$\Gamma_{\text{UV}}(L_{\text{eff}}) = \Gamma_{\infty}^{\text{UV}} + a^{\text{UV}} \exp(-2k^{\text{UV}} L_{\text{eff}}) \quad (5)$$

with fit parameters  $a^{\text{UV}}, k^{\text{UV}}$  and  $\Gamma_{\infty}^{\text{UV}}$ , we obtained well-converged decay-rate values  $\Gamma_{\infty}^{\text{UV}}({}^3_{\Lambda}\text{H} \rightarrow {}^3\text{He} + \pi^-)$ , as shown in Fig. 1 (lower panel) for several values of  $\Lambda_{\text{UV}} \geq 800$  MeV. This same procedure was applied, as shown in Fig. 1 (upper panel), to extrapolate  $E_{\text{g.s.}}({}^3_{\Lambda}\text{H})=E_{\text{d}}-B_{\Lambda}$ , with  $E_{\text{d}}$  the calculated free deuteron energy. The figure exhibits UV convergence for  $\Lambda_{\text{UV}} \geq 1$  GeV, with rates  $\Gamma_{\infty}^{\text{UV}}({}^3_{\Lambda}\text{H} \rightarrow {}^3\text{He} + \pi^-)=1.28 \pm 0.02$  GHz for  $B_{\Lambda}^{\text{UV}}({}^3_{\Lambda}\text{H})=0.162 \pm 0.003$  MeV. The corresponding extraction uncertainties are estimated as 1 keV for  $B_{\Lambda}$  and 3 MHz for  $\Gamma$ . Recalling the high-momentum cutoff scale  $\Lambda_{\text{QCD}} \sim M_B$ , for a  ${}^3_{\Lambda}\text{H}$  averaged baryon mass  $M_B \approx 1$  GeV, we chose to work with  $\Lambda_{\text{UV}}=1$  GeV.

The main contributions to  $\Gamma_{\infty}^{\text{UV}}({}^3_{\Lambda}\text{H} \rightarrow {}^3\text{He} + \pi^-)$  at  $\Lambda_{\text{UV}}=1$  GeV, for both PW and DW pions, are listed in Table 2. As seen, just three leading  ${}^3\text{He}$  and  ${}^3_{\Lambda}\text{H}$  configurations out of many other considered configurations reproduce within  $\lesssim 1\%$  uncertainty the total  ${}^3_{\Lambda}\text{H} \rightarrow {}^3\text{He} + \pi^-$  decay rate listed in the last row. Specifically, the dominant  $P({}^3_{\Lambda}\text{H})=96\%$  configuration in the first row corresponds to  $s_{\Lambda}$  hyperon coupled to a  ${}^3S_1$  quasi-deuteron that in  ${}^3\text{He}$  is close to the SU(4) limit of  $P=50\%$ . A few-percent  ${}^3D_1$  NN component induced by the tensor force in both  ${}^3\text{He}$  and  ${}^3_{\Lambda}\text{H}$  is added in the second row, almost saturating  $P({}^3_{\Lambda}\text{H})$ . About half of the remaining 0.8% probability arises from

Table 2: Partial decay rates  $\Gamma_{\infty}^{\text{UV}}(^3\Lambda\text{H}\rightarrow^3\text{He}+\pi^-)$  obtained by adding up fixed  $\Lambda_{\text{UV}}=1$  GeV contributions from three leading configurations in  $^3\text{He}$  and in  $^3\Lambda\text{H}$  are listed in GHz for PW and DW pions. Each of these  $l=0$  active-baryon ( $N, \Lambda, \Sigma$ ) configurations is specified by its spectator-nucleons isospin  $I$ , Pauli-spin  $S$ , orbital angular momentum  $L$  and total angular momentum  $J$ . Probabilities  $P$  are listed in percents. Total decay rates are given in the last row.

$^{(2I+1)(2S+1)}L_J$	$P(^3\text{He})$	$P_{\Lambda}(^3\Lambda\text{H})$	$P_{\Sigma}(^3\Lambda\text{H})$	$\Gamma_{\text{PW}}^{\text{UV}}$	$\Gamma_{\text{DW}}^{\text{UV}}$
$^{13}S_1$	46.81	95.87	–	1.141	1.310
$+^{13}D_1$	48.42	99.23	–	1.219	1.398
$+^{31}S_0$	94.87	99.23	0.14	1.108	1.266
$L \leq 7, I, S \leq 1$	100	99.61	0.39	1.099	1.265

$\Sigma NN$  configurations, induced by the  $\Lambda N \leftrightarrow \Sigma N$  transition component of the  $\chi\text{EFT } YN$  LO potential [23]. The leading such configuration, listed in the third row, is  $s_{\Sigma}$  hyperon coupled to a virtual-like  $^1S_0$   $NN$  component that in  $^3\text{He}$  is again close to the  $\text{SU}(4)$  limit of  $P=50\%$ . Remarkably, this tiny  $\Sigma NN$  admixture affects  $\Gamma_{\infty}^{\text{UV}}(^3\Lambda\text{H}\rightarrow^3\text{He}+\pi^-)$  more than the  $NN$  tensor force does, reducing the two-body decay rate by  $\approx 9\%$  as deduced by comparing the rates listed in the third row to those in the second row. The reduction is traced back to the sign of the  $\Lambda N \leftrightarrow \Sigma N$   $^1S_0$  contact term in the  $YN$  potential version used here; inverting this sign would reverse the sign of the observed charge symmetry breaking in the  $A=4$  hypernuclei [27]. The use of DW pions increases the PW two-body decay rate by  $\approx 15\%$ , inferred from the last row, higher than the  $\approx 10\%$  found in Ref. [12] where the pion optical potential was limited to its  $s$ -wave part; the larger DW effect found here owes to including its  $p$ -wave part. The two effects recorded here work in opposite directions, combining to a merely 3% increase of  $\Gamma_{\text{DW}}^{\Lambda+\Sigma}(^3\Lambda\text{H}\rightarrow^3\text{He}+\pi^-)$  with respect to  $\Gamma_{\text{PW}}^{\Lambda}(^3\Lambda\text{H}\rightarrow^3\text{He}+\pi^-)$  which is not listed here.

## 5. From $\Gamma(^3\Lambda\text{H}\rightarrow^3\text{He}+\pi^-)$ to $\tau(^3\Lambda\text{H})$

To get the inclusive  $\pi^-$  decay rate  $\Gamma_{\pi^-}(^3\Lambda\text{H})$  from the two-body decay rate  $\Gamma(^3\Lambda\text{H}\rightarrow^3\text{He}+\pi^-)$  we use the BC world average branching-ratio value  $R_3 = \Gamma(^3\Lambda\text{H}\rightarrow^3\text{He}+\pi^-)/\Gamma_{\pi^-}(^3\Lambda\text{H})=0.35\pm 0.04$  [14]. Note that decay tracks assigned to  $^3\Lambda\text{H}$  in BC experiments do not run the risk of resulting from decays of heavier hypernuclei in emulsion experiments where some of the tracks go unobserved and thereby potentially bias  $B_{\Lambda}$  determinations, such as the world



average value  $B_\Lambda(^3\Lambda\text{H})=0.13\pm 0.05$  MeV accepted by the hypernuclear community [40]. Applying this  $R_3$  to the two-body decay rate value 1.265 GHz associated in Fig. 1 with  $B_\Lambda(^3\Lambda\text{H})=159$  keV at  $\Lambda_{\text{UV}}=1$  GeV, and multiplying the obtained inclusive  $\Gamma_{\pi^-}(^3\Lambda\text{H})$  by the  $\Delta I = \frac{1}{2}$  factor  $\frac{3}{2}$  so as to include  $\Gamma_{\pi^0}(^3\Lambda\text{H})$ , the resulting pionic-decay  $^3\Lambda\text{H}$  lifetime is  $\tau_\pi(^3\Lambda\text{H})=184\pm 21$  ps, where the quoted uncertainty is statistical, arising from that of  $R_3$ . This calculated  $\tau_\pi(^3\Lambda\text{H})$  is shorter by  $(30\pm 8)\%$  than the free  $\Lambda$  lifetime  $\tau_\Lambda=263\pm 2$  ps. The total lifetime  $\tau(^3\Lambda\text{H})$  is shorter than that by (i)  $\approx 1.5\%$  from  $\Lambda N \rightarrow NN$  non-mesonic  $^3\Lambda\text{H}$  decay contributions [3, 41, 42]; and (ii)  $\approx 0.8\%$  from  $\pi NN \rightarrow NN$  pion true absorption in  $^3\Lambda\text{H}$  decay (mostly two-body) channels, estimated within our pion optical potential. The  $\approx 2.3\%$  summed yield of these non-pionic decay channels shortens slightly  $\tau_\pi(^3\Lambda\text{H})$ , leading to a  $^3\Lambda\text{H}$  lifetime  $\tau(^3\Lambda\text{H})=180\pm 21$  ps listed in the third row in Table 3. It was tacitly assumed throughout this derivation of  $\tau(^3\Lambda\text{H})$  that the branching ratio  $R_3$  used here, taken from experiment [14], indeed corresponds to  $B_\Lambda(^3\Lambda\text{H})=159$  keV at which the input  $\Gamma(^3\Lambda\text{H} \rightarrow ^3\text{He} + \pi^-)$  was evaluated.

Table 3: Two-body decay rates  $\Gamma(^3\Lambda\text{H} \rightarrow ^3\text{He} + \pi^-)$  (GHz) calculated for several  $\Lambda_{\text{UV}}$  cutoffs (MeV) from  $^3\Lambda\text{H}$  wavefunctions at given  $B_\Lambda$  values (keV), and as extrapolated to  $B_\Lambda=410$  keV, along with lifetimes  $\tau(^3\Lambda\text{H})$  (ps) evaluated using  $R_3=0.35\pm 0.04$  [14], the  $\Delta I = \frac{1}{2}$  rule, and an added 2.3% non-pionic decay rate.

$\Lambda_{\text{UV}}$	$B_\Lambda$	$\Gamma(^3\Lambda\text{H} \rightarrow ^3\text{He} + \pi^-)$	$\tau(^3\Lambda\text{H})$
800	69	0.975	$234\pm 27$
900	135	1.197	$190\pm 22$
1000	159	1.265	$180\pm 21$
–	410	1.403	$163\pm 18$

## 6. Relationship to $B_\Lambda$

Expecting a lifetime  $\tau(^3\Lambda\text{H})$  close to  $\tau_\Lambda$  for a weakly bound  $\Lambda$  hyperon in  $^3\Lambda\text{H}$ , one might worry why the present fully microscopic UV-converged two-body rate calculation at  $\Lambda_{\text{UV}}=1$  GeV yielded, when augmented by a branching ratio  $R_3$  from experiment, a pionic lifetime  $\tau_\pi(^3\Lambda\text{H})$  shorter than  $\tau_\Lambda$  by as much as  $\sim 30\%$ . In response we draw attention to the considerably lower two-body rates marked in Fig. 1 for  $\Lambda_{\text{UV}}=800, 900$  MeV, where UV convergence has not yet been fully achieved. This means that some UV corrections that depend on short-range details of the employed interactions are

missing in the extrapolation scheme of Eq. (5). Nevertheless, the correlation observed in the figure, for each value of  $\Lambda_{UV}$ , between  $\Gamma^{UV}({}^3_{\Lambda}\text{H} \rightarrow {}^3\text{He} + \pi^-)$  and its corresponding  $B_{\Lambda}^{UV}({}^3_{\Lambda}\text{H})$  appears robust. In particular the extrapolated two-body decay rates for  $\Lambda_{UV}=800, 900$  MeV provide meaningfully converged rates using well converged  ${}^3_{\Lambda}\text{H}$  wavefunctions with  $B_{\Lambda}^{UV}=69, 135$  keV respectively. Repeating for these two-body decay rates the procedure that led to a relatively short lifetime value in the third row of Table 3, using the same  $R_3$  value from experiment [14], we obtain for the least bound  ${}^3_{\Lambda}\text{H}$  case a value shorter than  $\tau_{\Lambda}$  by only  $\sim 11\%$ , as listed in first row of Table 3. This value of  $\tau({}^3_{\Lambda}\text{H})$  agrees reasonably with the latest published ALICE lifetime value [9] and, within its  $R_3$  induced uncertainty, also with Kamada *et al.*'s lifetime value derived in a fully three-body calculation, both listed in Table 1. Similarly, the lifetimes listed in the next two rows of Table 3 agree well within measurement uncertainties with the HypHI lifetime value listed in Table 1. Hence, as long as all  $B_{\Lambda}$  values within or close to the interval 0.07–0.16 MeV are acceptable, neither ALICE nor HypHI reported  ${}^3_{\Lambda}\text{H}$  lifetime values may be excluded. Given that the 50 keV uncertainty in the cited value  $B_{\Lambda}({}^3_{\Lambda}\text{H})=0.13\pm 0.05$  MeV [2] is purely statistical, and that a systematic uncertainty of the same size is plausible, a conservative estimate of the combined uncertainty is 0.07 MeV, so that all values of  $B_{\Lambda}({}^3_{\Lambda}\text{H})$  between 0.06 and 0.20 MeV are acceptable, and so are both ALICE's and HypHI's lifetime values.

To discuss more quantitatively STAR's reported  $\tau({}^3_{\Lambda}\text{H})$  we extrapolate  $\Gamma({}^3_{\Lambda}\text{H} \rightarrow {}^3\text{He} + \pi^-)$  from the calculated values listed in the first three rows of Table 3 to a decay-rate value appropriate to  $B_{\Lambda}({}^3_{\Lambda}\text{H})=0.41$  MeV, STAR's mean value claimed recently:  $B_{\Lambda}({}^3_{\Lambda}\text{H})=0.41\pm 0.12\pm 0.11$  MeV [16]. Expanding  $\Gamma({}^3_{\Lambda}\text{H} \rightarrow {}^3\text{He} + \pi^-)$  in powers of  $\sqrt{B_{\Lambda}}$ , with just linear and quadratic terms, we derive a value  $\Gamma({}^3_{\Lambda}\text{H} \rightarrow {}^3\text{He} + \pi^-)$  for  $B_{\Lambda}({}^3_{\Lambda}\text{H})=0.41$  MeV, as listed in the last row of the table. Repeating the procedure explained above of obtaining  $\tau({}^3_{\Lambda}\text{H})$ , we get  $163\pm 18$  ps which has substantial overlap with STAR's reported lifetime [7] listed in Table 1. In fact, had we used STAR's central value  $R_3=0.32$  from their own observation of  ${}^3_{\Lambda}\text{H}$  two-body and three-body  $\pi^-$  decays,  $R_3=0.32\pm 0.05\pm 0.08$  [7], we would have obtained  $\tau({}^3_{\Lambda}\text{H})=149$  ps, almost coincident with STAR's central lifetime value listed in Table 1.

## 7. Concluding Remarks

Reported in this work is a new microscopic three-body calculation of the  ${}^3_{\Lambda}\text{H}$  pionic two-body decay rate  $\Gamma({}^3_{\Lambda}\text{H} \rightarrow {}^3\text{He} + \pi^-)$ . Using the  $\Delta I = \frac{1}{2}$  rule and a branching ratio  $R_3$  from experiment to connect to additional pionic decay rates, the lifetime  $\tau({}^3_{\Lambda}\text{H})$  was deduced. As emphasized here  $\tau({}^3_{\Lambda}\text{H})$  varies strongly with the small, rather poorly known  $\Lambda$  separation energy  $B_{\Lambda}({}^3_{\Lambda}\text{H})$ ; it proves possible then to correlate each one of the three distinct RHI experimentally reported values  $\tau_{\text{exp}}({}^3_{\Lambda}\text{H})$  with a theoretical value  $\tau_{\text{th}}({}^3_{\Lambda}\text{H})$  that corresponds to its own underlying  $B_{\Lambda}({}^3_{\Lambda}\text{H})$  value. The  $B_{\Lambda}({}^3_{\Lambda}\text{H})$  intervals thereby correlated with these experiments are roughly  $B_{\Lambda} \lesssim 0.1$  MeV,  $0.1 \lesssim B_{\Lambda} \lesssim 0.2$  MeV and  $B_{\Lambda} \gtrsim 0.2$  MeV for ALICE, HypHI and STAR, respectively. New experiments proposed at MAMI on Li target [43] and at JLab, J-PARC and ELPH on  ${}^3\text{He}$  target [44] will hopefully pin down precisely  $B_{\Lambda}({}^3_{\Lambda}\text{H})$  to better than perhaps 50 keV, thereby leading to a unique resolution of the ‘hypertriton lifetime puzzle’.

## Acknowledgments

We are grateful to Patrick Achenbach, Nir Barnea, Peter Braun-Munzinger, Benjamin Dönigus, Alessandro Feliciello, Hans-Werner Hammer, Jiří Mareš and Satoshi Nakamura for useful remarks on a previous version. The work of DG was supported by the Czech Science Foundation, GAČR grant No. 19-19640S. Furthermore, the work of DG, EF and AG was partially funded by the European Union’s Horizon 2020 research & innovation programme, grant agreement 824093.

## References

- [1] A. Gal, E.V. Hungerford, D.J. Millener, *Rev. Mod. Phys.* 88 (2016) 035004.
- [2] D.H. Davis, *Nucl. Phys. A* 754 (2005) 3c.
- [3] M. Rayet, R.H. Dalitz, *N. Cimento* 46A (1966) 786.
- [4] [www.pdglive.lbl.gov](http://www.pdglive.lbl.gov), 2020 Review of Particle Physics, P.A. Zyla, et al. (Particle Data Group), *Prog. Theor. Exp. Phys.* 2020 (2020) 083C01.

- [5] C. Rappold, et al. (HypHI Collaboration), Nucl. Phys. A 913 (2013) 170.
- [6] B.I. Abelev, et al. (STAR Collaboration), Science 328 (2010) 58.
- [7] L. Adamczyk, et al. (STAR Collaboration), Phys. Rev. C 97 (2018) 054909.
- [8] J. Adam, et al. (ALICE Collaboration), Phys. Lett. B 754 (2016) 360.
- [9] S. Acharya, et al. (ALICE Collaboration), Phys. Lett. B 797 (2019) 134905.
- [10] A preliminary value  $\tau(^3_\Lambda\text{H})=254\pm 15\pm 17$  ps was presented by F. Mazzaschi on behalf of the ALICE Collaboration, CERN, at the ICHEP 2020, Prague, 31/07/2020 (<https://indico.cern.ch/event/868940/contributions/>).
- [11] H. Kamada, J. Golak, K. Miyagawa, H. Witała, W. Glöckle, Phys. Rev. C 57 (1998) 1595.
- [12] A. Gal, H. Garcilazo, Phys. Lett. B 791 (2019) 48.
- [13] F. Hildenbrand, H.-W. Hammer, arXiv:2007.10122v1, submitted to Phys. Rev. C (2020).
- [14] G. Keyes, J. Sacton, J.H. Wickens, M.M. Block, Nucl. Phys. B 67 (1973) 269.
- [15] P. Liu (for the STAR Collaboration), Nucl. Phys. A 982, 811 (2019); showing two preliminary  $^3_\Lambda\text{H}$  invariant mass distributions reconstructed from two-body and three-body decay channels, from which apparently the STAR [16] overall  $B_\Lambda(^3_\Lambda\text{H})$  value was extracted. Note however that the separate  $^3_\Lambda\text{H}$  invariant mass distributions appear mutually exclusive of each other.
- [16] J. Adam, et al. (STAR Collaboration), Nature Physics 16 (2020) 409.
- [17] H. Le, J. Haidenbauer, U.-G. Meißner, A. Nogga, Phys. Lett. B 801 (2020) 135189.
- [18] D. Logoteta, I. Vidaña, I. Bombaci, Eur. Phys. J. A 55 (2019) 207.

- [19] D. Gerstung, N. Kaiser, W. Weise, Eur. Phys. J. A 56 (2020) 175.
- [20] L. Tolos, L. Fabbietti, Prog. Part. Nucl. Phys. 112 (2020) 103770.
- [21] P.M.M. Maessen, T.A. Rijken, J.J. de Swart, Phys. Rev. C 40 (1989) 2226.
- [22] A. Nogga, H. Kamada, W. Glöckle, Phys. Rev. Lett. 88 (2002) 172501.
- [23] H. Polinder, J. Haidenbauer, U.-G. Meißner, Nucl. Phys. A 779 (2006) 244.
- [24] J. Haidenbauer, U.-G. Meißner, A. Nogga, H. Polinder, in *Topics in Strangeness Nuclear Physics*, Eds. P. Bydžovský, A. Gal, and J. Mareš, Lecture Notes in Physics 724 (2007) 113-140.
- [25] A. Nogga, Nucl. Phys. A 914 (2013) 140.
- [26] D. Gazda, J. Mareš, P. Navrátil, R. Roth, R. Wirth, Few-Body Syst. 55 (2014) 857.
- [27] D. Gazda, A. Gal, Phys. Rev. Lett. 116 (2016) 122501, and Nucl. Phys. A 954 (2016) 161.
- [28] M. Ablikim, et al. (The BESIII Collaboration), Nature Physics 15 (2019) 631; see also the pdgLive compilation [4].
- [29] J.F. Donoghue, E. Golowich, B.R. Holstein, *Dynamics of the Standard Model*, second edition (Cambridge University Press, Cambridge UK, 2014).
- [30] E. Friedman, A. Gal, Phys. Rep. 452 (2007) 89.
- [31] E. Friedman, A. Gal, Nucl. Phys. A 928 (2014) 128.
- [32] E. Friedman, A. Gal, Phys. Lett. B 792 (2019) 340.
- [33] E. Friedman, A. Gal, Acta Phys. Pol. B 51 (2020) 45.
- [34] I. Schwanner, G. Backenstoss, W. Kowald, L. Tauscher, H.-J. Weyer, D. Gotta, H. Ullrich, Nucl. Phys. A 412 (1984) 253.

- [35] R.A. Arndt, W.J. Briscoe, I.I. Strakovsky, R.L. Workman, Phys. Rev. C 74 (2006) 045205; see also SAID program <http://gwdac.phys.gwu.edu/>
- [36] E. Friedman, et al., Phys. Rev. Lett. 93 (2004) 122302, and Phys. Rev. C 72 (2005) 034609.
- [37] B.D. Carlsson, A. Ekström, C. Forssén, D.F. Strömberg, G.R. Jansen, O. Lilja, M. Lindby, B.A. Mattsson, K.A. Wendt, Phys. Rev. X 6 (2016) 011019.
- [38] R. Wirth, D. Gazda, P. Navrátil, R. Roth, Phys. Rev. C 97 (2018) 064315.
- [39] C. Forssén, B.D. Carlsson, H.T. Johansson, D. Sääf, A. Bansal, G. Hagen, T. Papenbrock, Phys. Rev. C 97 (2018) 034328.
- [40] M. Jurič, et al., Nucl. Phys. B 52 (1973) 1.
- [41] J. Golak, K. Miyagawa, H. Kamada, H. Witała, W. Glöckle, A. Parreño, A. Ramos, C. Bennhold, Phys. Rev. C 55 (1997) 2196; Erratum: 56 (1997) 2892.
- [42] A. Pérez-Obiol, D.R. Entem, A. Nogga, J. Phys. Conf. Proc. Series 1024 (2018) 012033.
- [43] P. Achenbach, S. Bleser, J. Pochodzalla, M. Steinen, PoS **Hadron2017** (2018) 207.
- [44] S.N. Nakamura, AIP Conf. Proc. 2130 (2019) 020012; A. Feliciello, AIP Conf. Proc. 2130 (2019) 020020.